

Medium Access and Transport Protocol Aspects in Practical 802.11ad Networks

Hany Assasa^{*†}, Swetank Kumar Saha[‡], Adrian Loch[†], Dimitrios Koutsonikolas[‡] and Joerg Widmer[†]

Universidad Carlos III de Madrid, Spain^{*}

IMDEA Networks Institute, Madrid, Spain[†]

University at Buffalo, SUNY, US[‡]

Email: {hany.assasa, adrian.loch, joerg.widmer}@imdea.org, {swetankk, dimitrio}@buffalo.edu

Abstract—The use of directional antennas in millimeter-wave communication promises high spatial reuse at multi-gigabit-per-second data rates in dense wireless networks. Existing work studies such networks using commercial hardware but is limited to individual links. Moreover, such hardware typically allows for little or no control of the lower layers of the protocol stack. In this paper, we study the performance of dense millimeter-wave deployments featuring up to eight stations. To this end, we use a practical IEEE 802.11ad millimeter-wave testbed that allows access to the lower layer parameters of each station. This enables us to analyze the impact of these parameters on upper layer performance. We study, for first time to our best knowledge, issues such as the impact of channel contention on the buffer size at the transport layer, the effect of frame aggregation, and the efficiency of spatial sharing. Our results show that using large buffer sizes with TCP is harmful due to channel contention despite the multi-gigabit-per-second data rates. Further, frame aggregation is only beneficial up to a certain level due to higher error rates for large frames. Finally, we also study delay, showing that the regular beacon transmission time can degrade performance.

I. INTRODUCTION

Millimeter-wave (mmWave) communications narrow the gap between wired and wireless networks. While both domains are fundamentally different, mmWave wireless networks feature highly directional links and large bandwidths which result in low interference and high throughput, similarly to the wired case. Early work in this area even dubs mmWave links as “pseudo-wired” [1]. Such links can alleviate the characteristics of wireless links that hinder the seamless integration with the wired part of the network. For instance, the limited interference results in less random packet losses, which in turn improves the operation of the Transmission Control Protocol (TCP) that would otherwise interpret such losses as congestion [2]. Also, directional links are less prone to fluctuations due to changing reflections, yielding high and stable throughput as in the wired case.

On the other hand, some of the features of mmWave links are still inherently wireless. For example, packet loss can still be high due to the inherent characteristics of the wireless medium triggering link adaptation algorithms (rate adaptation, beamforming); and mmWave access points (APs) still transmit beacons to allow clients to discover them, which may interfere with data transmission. More importantly, practical phased

array antennas in commercial off the shelf (COTS) devices typically generate wide beam patterns with strong side lobes instead of perfect “pencil beams” [3], [4]; such patterns can increase interference among neighboring links. Thus, the characteristics of mmWave links correspond neither to the ones of wired links nor to the ones of traditional wireless links. To date, it is not well understood how such links with mixed characteristics behave in practical WLAN deployments.

In this paper, we fill this gap by studying the practical performance of 60 GHz WLANs comprised of COTS APs and clients. Earlier work in this area is limited to isolated mmWave links [5], [3], [6], [7], whereas we consider a complete network with up to eight stations that fully complies to the IEEE 802.11ad standard [8]. Moreover, we extract detailed information regarding the operation of the network across all layers of the protocol stack directly from our 802.11ad hardware. To this end, we install LEDE [9] on a COTS router operating in the 60 GHz band. In contrast, earlier work has no access to the inner workings of 802.11ad hardware and thus can only conjecture regarding the effects it measures. This allows us to obtain unprecedented insights into the operation of mmWave networks for the case of 802.11ad. As a result of the aforementioned mixed characteristics of mmWave links, many of those insights are unexpected and challenge the prevailing intuition regarding communication links. Specifically, our insights are as follows:

- 1) The very high data rates in mmWave networks exacerbate the inefficiencies of CSMA/CA resulting in strong link fluctuations. Thus, dynamic TCP buffer sizing [10] is crucial and much more relevant than in wireless networks operating in the 2.4 GHz and 5 GHz bands. The deafness due to the need for directional communication in the mmWave band further worsens this issue.
- 2) The susceptibility of mmWave to blockage and human mobility requires frequent beamforming training and tracking to avoid link interruption. This signaling overhead exacerbates in large dense deployments with many clients and degrades as a result the performance of the downlink TCP flows. This requires either good network planning to distribute clients among access point to reduce potential blockages or intelligent tracking methods to exchange less messages when establishing a com-

munication link. We highlight this effect in section III as this behavior did not exist for WLAN networks operating below 6 GHz.

- 3) While mmWave frame aggregation is highly beneficial to limit the impact of medium access overhead, the packet error rate increase due to high aggregation levels is much more pronounced than for traditional wireless and wired networks. The former supports aggregation up to ten milliseconds and the latter in the form of very large “jumbo frames”. In contrast, mmWave links are limited to frame aggregation in the order of microseconds [3].
- 4) The beacons that 802.11ad APs transmit on each of their beam patterns periodically to enable highly directional communication can interact with data transmissions. As a result, we observe spikes in the Round Trip Time (RTT) which in turn influences the behavior of TCP and may cause the above unfairness. Other effects, such as increased backbone delays, result in the same issues.
- 5) Link orientation plays a large role regarding whether two links can operate simultaneously. In wired networks this is irrelevant, since links only interfere in case of cross-talk among densely packed cables. This also does not apply for traditional wireless networks, where interference is only related to the distance among nodes.

This paper is structured as follows. In Section II we explain our experimental methodology. After that, in Sections VI to V we present our results on spatial sharing, Carrier Sense Multiple Access with Collision Avoidance (CSMA/CA) behavior, frame aggregation, and delay, respectively. In Section VIII we survey related work in the field of practical mmWave hardware. Finally, Section IX concludes the paper.

II. EXPERIMENTAL METHODOLOGY

In this section, we list the set of devices that we use and then present our WLAN setup.

A. Devices

The **TP-Link Talon AD7200** [11] was the first commercially available 802.11ad router released in June 2016. For 802.11ad, it uses the QCA9008-SBD1 module with the QCA9500 chipset from Qualcomm, supporting single-carrier data rates up to 4.6 Gbps. The 32-element phased antenna array is located on a separate board and connected to the chipset with a MHF4 cable. The router also includes a 802.11n/ac solution from Qualcomm. Since it only provides 1G Ethernet, maximum throughput is limited to 1 Gbps.

The **Netgear Nighthawk X10 Smart WiFi Router** [12] was released around October 2016. It uses the same module from Qualcomm for 802.11ad as the one used by Talon. In addition to the 1G Ethernet ports, it has a 10-Gigabit LAN SFP+ interface. While the 10G port theoretically provides multi-Gigabit speeds, we found that in practice the maximum throughput (with MCS 12) is limited to around 2.3 Gbps.

The **Acer Travelmate P446-M** [13] laptop, released in April 2016, has the client-version QCA9008-TBD1 of the module used in the Nighthawk and Talon routers, which

includes 802.11ac, 802.11ad and Bluetooth chipsets. The host connects to the module using an M.2 slot, runs Linux OS (Fedora 24, kernel 4.x) and uses the open source wil6210 wireless driver to interface with the chipset. It comes with same 32-element phased antenna array as the routers.

B. Measurement Methodology

We differentiate between three sets of experiments based on the number of clients. The first set (Sections III, VI) uses multiple Talon routers, some setup in AP mode and the rest in client mode to have a WLAN-like environment. The second set of experiments (Section IV) uses again a router in AP mode and a laptop in client mode but there is no desktop connected to the router. Finally, the third set of experiments (Section V) consists of a router running in AP mode connected over a 1G Ethernet link to a high-end desktop and a laptop operating in client mode and associated to that AP. In the first and second set of experiments, we flash LEDE [14] on the Talon routers – a Linux operating system based on OpenWrt. This allows us to manage these routers and collect measurement performance in a centralized way. For these routers, we either use the Ethernet interface or the 2.4/5 GHz WLAN interface for management and control. Note that the driver, firmware, chipset, and the phased antenna array in the Talon router in this case is the same as in the laptop.

The Wilocity driver (wil6210) available in Linux operating systems allows to set the device in either AP mode, monitor mode, or client mode. In addition, it provides some useful information regarding the wireless link such as the current MCS, MAC layer throughput, Signal quality indicator (SQI), Beamforming Training Status (OK/Failed/Retrying), Tx/RX sector IDs for itself and the peer device, and the number of received packets per MCS. We log all the parameters every 150 ms. The current Wilocity firmware “3.3.3.7759” implements both a proprietary beamforming algorithm for selecting the best transmit sector and a rate adaptation mechanism for MCS selection. As a result, it does not allow fixing either the MCS or transmit/receive sector IDs.

We use iPerf2, a network benchmarking tool, for generating TCP/UDP traffic. Unless otherwise stated, the reporting period of iPerf is 100 ms. When using TCP with iPerf, iPerf reports the throughput, the round-trip time (RTT), and the congestion window (CWND). Each iPerf session last for 60 seconds and all the results are averaged over 50 to 10 runs.

III. BEHAVIOR OF CSMA/CA

Current studies on WiGig and 802.11ad in the literature focus on characterizing and benchmarking the performance of a single communication link for different placements and in different scenarios [3]. While they provide valuable insights, it is very important to move one step further and study the performance of COTS 802.11ad enabled devices in large, dense deployments, i.e., WLAN setups. In addition, these studies ignore the interaction between the protocol aspects of the IEEE 802.11ad standard and the operations of the transport protocols such as TCP. In this section, we try to answer

the following questions: i) how would 802.11ad enabled devices share the wireless medium? ii) What is the impact of transport layer buffering on the perceived throughput, latency, and fairness between competing TCP flows? iii) What is the optimal size for TCP buffer? iv) How does the directionality in mmWave networks impact the performance of transport layer protocols? To answer these questions, we carry out extensive measurement campaigns where we deploy eight stations and a single AP within a room of size 6x3x5 meters as shown in Figure 1. All the stations are placed at the same height and each one starts a single TCP flow at the same time towards the AP, or receives a single TCP flow from the AP. Each experiment lasts for 60 seconds and we repeat each experiment between 5 to 10 times. We differentiate between two scenarios based on the direction of the TCP flows, namely uplink or downlink.



Fig. 1. Dense Deployment Setup Layout.

A. Downlink Scenario

In the downlink scenario, the AP generates single bulk TCP flow towards each station. This scenario mimics the case of fetching large file from a NAS storage device over a wireless gigabit link. The frequent channel access here comes mainly from the AP, since it has to multiplex transmissions among several stations. Thus, the impact of the stations contending to transmit TCP ACKs back to the AP is minimal compared to the channel contention required to transmit the high amount of TCP data segments to those stations. In fact, this gives us a high degree of flexibility to isolate the interactions between TCP behavior and CSMA/CA protocol aspects. Moreover, this allows us to understand the impact of Linux TCP receive buffer size on the aggregated throughput and the measured RTT time.

Figure 2 shows the aggregated throughput for all the flows with respect to the number of stations and for various TCP receive buffer sizes. By default, LEDE uses 4 MBytes for the size of both TCP send and receive buffers. We benchmark the performance using additional values for the TCP receive buffer size: a small value (1 Mbytes), the default value (4 MBytes), and a large value (32 MBytes). For a fixed number of stations, the throughput increases proportionally with the size of the TCP buffer. For 6 and 8 stations, the throughput starts to stabilize for each buffer size values. However, the most important observation here is that the aggregate throughput drops with the number of stations. This is due to the inefficiencies of CSMA/CA. Additionally, due to the nature of the mmWave, stations cannot distinguish if a packet loss

is due to collision, deafness, or shadowing. For that reason, a station tries frequently to access the wireless medium in order to perform beamforming training with the corresponding peer station. This is a further reason why the aggregated throughput degrades with increasing number of stations. This additional overhead that does not exist for wireless networks operating in the microwave band. There are numerous experimental and analytical studies [15], [16], [17], [18] that study and evaluate TCP performance in dense WLAN settings in the microwave band. All of these studies show that TCP downlink throughput scales quite well with increasing number of clients if stations do not generate any uplink traffic. For 802.11ad networks, stations have to access the channel occasionally to perform beamforming training even if they do not have any data for transmission.

Figure 3 depicts the average RTT for all the flows. The RTT rises as we increase both the number of stations and TCP buffer size. This is due to the fact that the AP has to multiplex between different flows, which results in queue building up at the wireless interface of the AP. In addition, the contention of the returning TCP ACKs and the frequent beamforming training play a role in the rise of the RTT. As a result, efficient methods for enabling fast beam alignment are key aspects in the design of mmWave protocols since the overhead of beamforming training has a clear impact on the performance of TCP in the downlink.

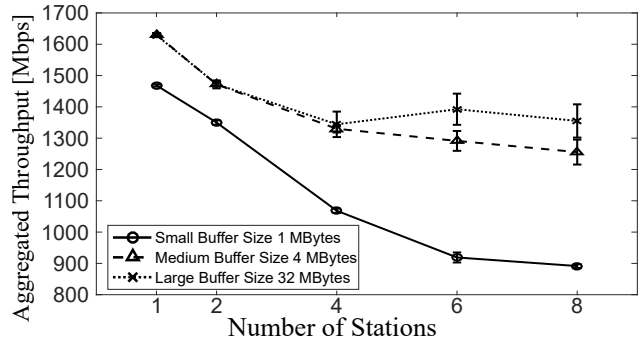


Fig. 2. Aggregated Throughput Comparison for Downlink Scenario.

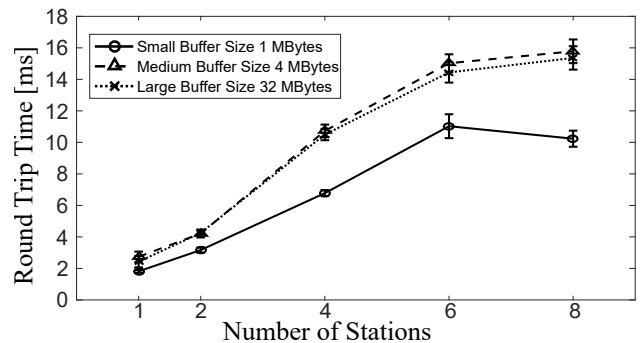


Fig. 3. RTT Comparison for Downlink Scenario.

B. Uplink Scenario

In contrast to the downlink scenario where a single station contends frequently to access the channel, the uplink scenario comprises multiple stations trying to access the channel to transmit their data towards the AP. As a result, CSMA/CA has a direct impact on the performance of the transport protocol and the amount of buffering in the transport layer. Similar to the downlink scenario, we study the impact of the size of TCP receive and send buffers together with the number of contending stations on the achievable throughput and RTT. Additionally, we study Jain's fairness index to have a better understanding on the fairness between the TCP flows. Jain's fairness index ranges between 0.125 and 1; 0.125 is the lowest value corresponding to completely unfair channel allocation whereas 1 means that the allocation scheme is fair and all the flows share the bandwidth equally.

Figure 4 shows that using a large TCP buffer for high contention scenarios improves the total aggregated throughput. A large buffer masks the channel changes which are more frequent in the 60 GHz band but this comes at the expense of increasing the RTT as can be seen in Figure 5. The RTT is almost 5 to 10 times fold compared to the downlink scenario even for a small number of stations and with small TCP buffer size.

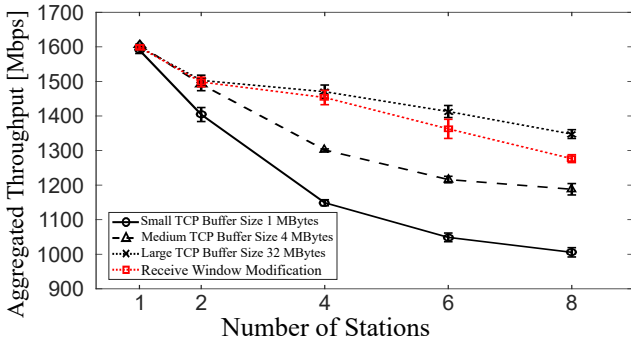


Fig. 4. Aggregated Throughput Comparison for Uplink Scenario.

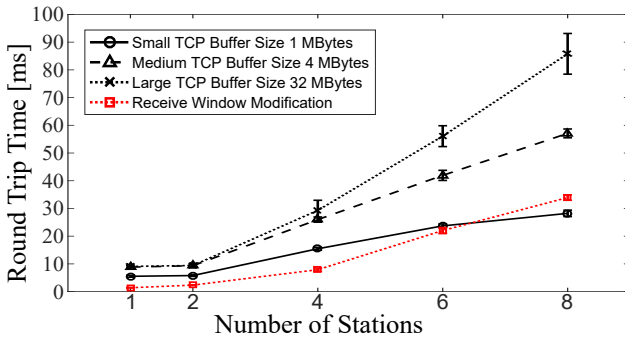


Fig. 5. RTT Comparison for Uplink Scenario.

We plot Jain's fairness index in Figure 6 with a confidence interval of 95% with respect to the fairness window. The

fairness window refers to a moving mean that varies from 100 ms to 3 s. The variable size of the moving mean captures after how much time flows start sharing the wireless medium fairly and efficiently. If Jain's index is very high for a small window size, this means that all the clients are using the channel fairly and none of them is starving. On the other hand, if Jain's index becomes high for a very large window size, this implies that at some instance of time, some of the flows are fully blocked and only get served after waiting for some time.

For a small number of stations, Jain's index is high even for small fairness window sizes. Fairness among flows decreases when we increase both the number of active stations and the size of TCP buffer even for a fairness window of 3 s. This is true especially for the case of a large buffer size. To understand the reason behind this low fairness, we look at the instantaneous throughput variation for eight stations in Figure 7(a). We observe that TCP is very aggressive and the instantaneous throughput can reach up to 1 Gbps. In addition, some stations have gaps of zero throughput; those stations were idle for a couple of hundreds of milliseconds since the wireless medium is highly utilized. Because of that each station starts to buffer packets until it get a transmission opportunity, which increases the round trip time and decreases fairness between the flows.

To avoid excessive buffering, we need to set the congestion window size at the sender side to the actual size of the bandwidth delay product (BDP). For this purpose, we rely on the idea of receive size window modification to set the optimum value of the BDP and thus solving the problem of high RTT while achieving high throughput. The receiver window sizing has been already proposed to mitigate the buffer bloat problem in cellular networks [19]. By definition, the $BDP = \text{Bottleneck Capacity} * \text{Base RTT}$. The Base RTT corresponds to the lowest value observed in the same system without buffering. If we set the CWND to a value higher than the BDP then queues start to build up inside the network. However, in our setup the optimum BDP value depends on the number of the contending stations since the CSMA/CA part contributes to the RTT as high number of contending stations results in an increased channel access delay per station.

We take the value of the lowest RTT from Figure 5, which corresponds to the smallest buffer size, and we use it as the base RTT. For the bottleneck capacity or the desirable throughput, we take the value of the highest aggregated throughput in Figure 4 for large buffer size and divide it by the number of stations. We use these values to set the receive window size at the AP and we plot again the RTT, aggregated throughput, and Jain's fairness index. Figures 5, 4, and 6 show the performance of the receive window modification. The performance becomes drastically better. For a different number of stations we can achieve almost a throughput similar to the case of large buffer size but with much lower latency. Figure 7(b) shows the instantaneous throughput after modifying the receive window size. TCP becomes less aggressive and the throughput becomes significantly smoother over the period of during the communication. As a result, setting the TCP buffer

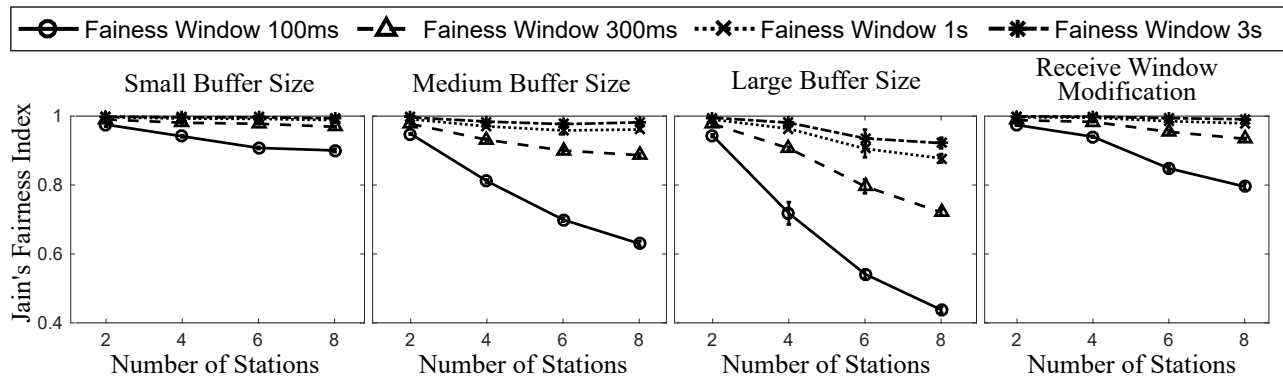


Fig. 6. Fairness Comparison for Uplink Scenario.

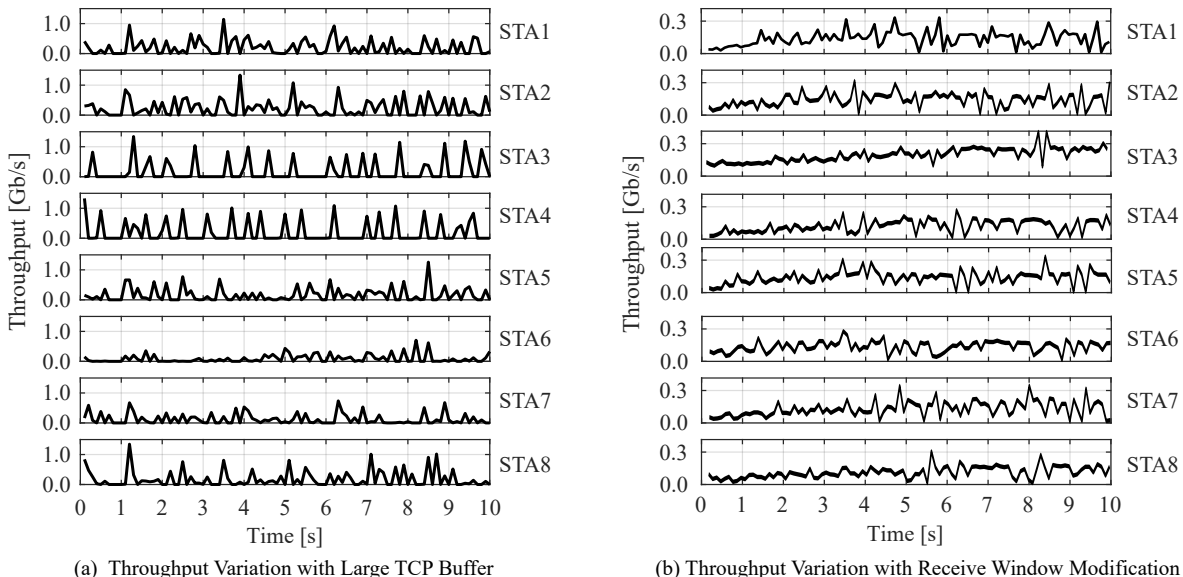


Fig. 7. IPERF Throughput Variation for 8 Stations with Large Buffer Size.

size to the actual BDP, prevents TCP from pushing burst of packets into the MAC layer and causing sequential timeouts. This increases the RTT by a factor of 3x.

The only reasonable solution for a station to obtain the maximum throughput in the uplink case even if it is alone is to set the TCP send buffer large enough. However, due to the inefficiencies of the CSMA/CA protocol, a large buffer makes TCP aggressive and causes unfairness between flows in the case of high contention. We cannot adapt the transmit buffer at the station since it requires the station to estimate the number of other stations in the wireless network. Since millimeter-wave networks use directional antennas, the estimation becomes hard due to deafness. However, it is possible to the AP since it is aware of all the stations that are connected and sees the flows of all the stations; thus, it can determine the right per flow rate. This means that the AP can perform the receive window overwriting so it can throttle the flows that are too aggressive and cause high medium utilization with CSMA/CA.

Another solution is that the AP can use a scheduled channel access scheme (TDMA) to assign slots for each station. In this way, a station can determine the exact flow rate during its time slot. However, the current firmware running on the 802.11ad chipset is limited to CSMA/CA operation.

IV. FRAME AGGREGATION

802.11ad, like its predecessors 802.11n/ac, allows for both A-MSDU and A-MPDU aggregation to improve MAC efficiency. While the A-MSDU aggregation is limited to 7935 bytes, a station using A-MPDU aggregation can aggregate either up to 64 packets or up to 262143 bytes as long as the length of the frame does not exceed 2 ms. Although both A-MSDU and A-MPDU aggregation can be combined together to further increase MAC efficiency, the chipset firmware used by our devices only supports A-MPDU aggregation with either a window size of at most 32 packets or up to 65536 bytes.

In this section, we analyze the impact of changing aggregation window size on the achievable MAC throughput. In

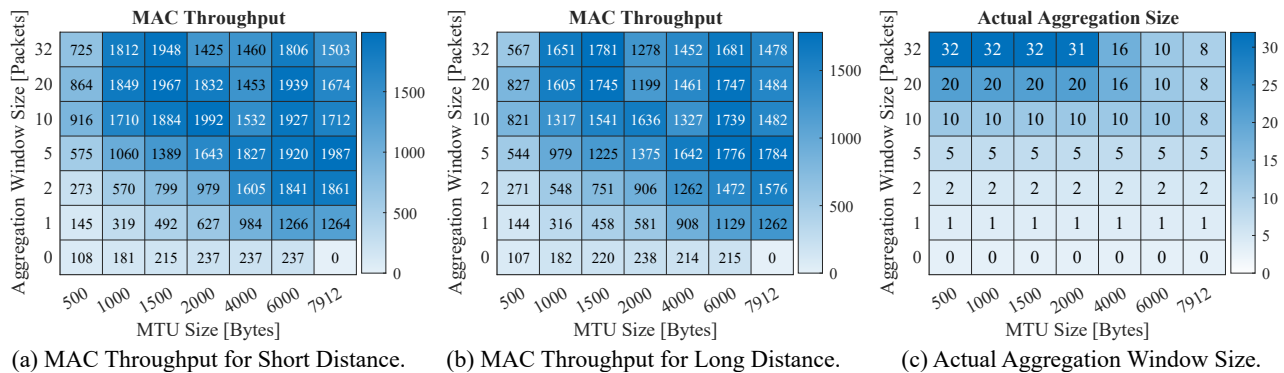


Fig. 8. A-MPDU Aggregation Performance in wil6210.

addition, we emulate the behavior of A-MSDU aggregation by varying the maximum MTU size of the support (wil6210 driver supports MTU size of up to 7912 bytes). We use UDP traffic in the uplink direction, with a packet size always kept smaller than the maximum MTU size to avoid IP fragmentation. We enable the `rx_large_buf` parameter in the wil6210 driver to allocate a large buffer for high MTU values.

We perform these measurements in two different settings. In the first setting, we place the laptop in close proximity to the AP (Small Distance Setting), whereas the second setting corresponds to a 9 m separation between the laptop and the AP (Long Distance Setting). Figures 8 (a) and (b) depict the heat map of the achievable MAC throughput for different MTU values and aggregation window sizes. Note that, since the current firmware limits the number of bytes that can be aggregated, the actual window size is practically smaller than the set window size. Figure 8 (c) depicts the actual window size for all combinations of set window size and MTU size based on wil6210 driver.

One would expect that increasing MTU and aggregation window sizes would lead to throughput increase. However, we observe that some combinations of MTU sizes and aggregation window sizes in fact degrade the performance. This is because a large aggregation window size or frame size increases the probability of having erroneous sub-frames inside an A-MPDU frame. Erroneous frames trigger the rate adaptation mechanism to lower its current MCS to cope with instantaneous channel changes. Figure 9 shows the distribution of MCSs for an MTU size of 2000 bytes for different aggregation window sizes in the small distance setting. We can see that for an aggregation window size of 20 and 32 frames, we have a high occurrence of both MCSs 8 and 11 compared to the case of aggregation window size of 10 frames. This gives an indication that rate adaptation algorithm try to use MCS 11 for its transmission. However, due to the high probability of error with a large aggregated packet, the rate adaptation mechanisms lowers its current MCS and utilizes MCS 8 more frequently which results in throughput degradation.

Interestingly, for both short and long distances, Figures 8 (a) and (b) show two areas of maximum throughput: (i)

large MTU sizes (6000 bytes or more) and small to medium aggregation window size (5-20) and (ii) the default MTU size (1500 bytes) and large aggregation window sizes (20-32). In contrast, the combination of maximum MTU and aggregation window size yields lower throughput.

Note that for an MTU size of 7912 bytes with A-MPDU aggregation disabled, we were unable to establish communication with the AP. Further, setting the aggregation window size to 0 disables A-MPDU frame aggregation in the firmware. Interestingly, if we set the aggregation window size to a single packet we achieve higher throughput compared to the case of disabled aggregation. The reason is that when we set the aggregation window size to a value equal to or larger than one packet, the firmware enables the Transmission Opportunity (TxOP) feature that allows a station to hold the wireless medium for certain amount of time depending on traffic class.

V. DELAY

The analysis in the previous sections focused largely on achievable throughput. However, for many applications like web-browsing, RTT matters more than throughput in determining the user-perceived delay. Here, using the first of the two setups described in Section II-B and ICMP ping packets, we measure the RTT between the laptop and the host machine attached directly to the AP. We experimented with both routers in various indoor locations. In the interest of space, we only present the results with Nighthawk at one location but other router-location combinations gave similar results.

Figure 10(a) shows the mean RTT for 100 ICMP REQUEST-REPLY pairs, with a 1 s interval between two consecutive REQUESTs, as measured at different distances between the AP and the client. The mean RTT at all distances is longer than 40 ms. Additionally, all distances show large variance in the RTT, with RTTs as large as 100 ms and as small as 3 ms. These values, undoubtedly, are too high for a WLAN setup involving two fast links (802.11ad and 10G Ethernet). In fact, the RTTs to the same host when reached through the 802.11ac interface were always lower than 2 ms, indicating that the issue is unique to the 802.11ad path. We repeated our measurements with a single-hop ping to the router

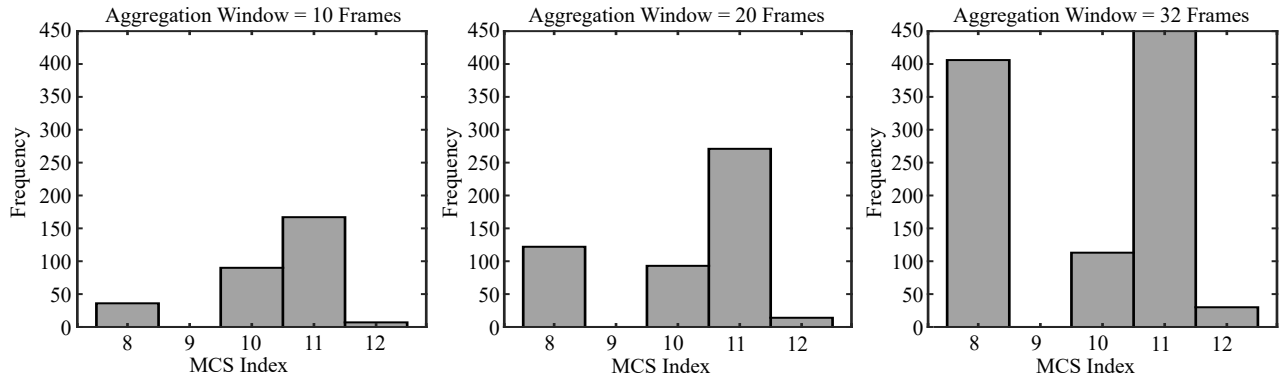


Fig. 9. MCSs Distribution for Small Distance with MTU = 2000 Bytes.

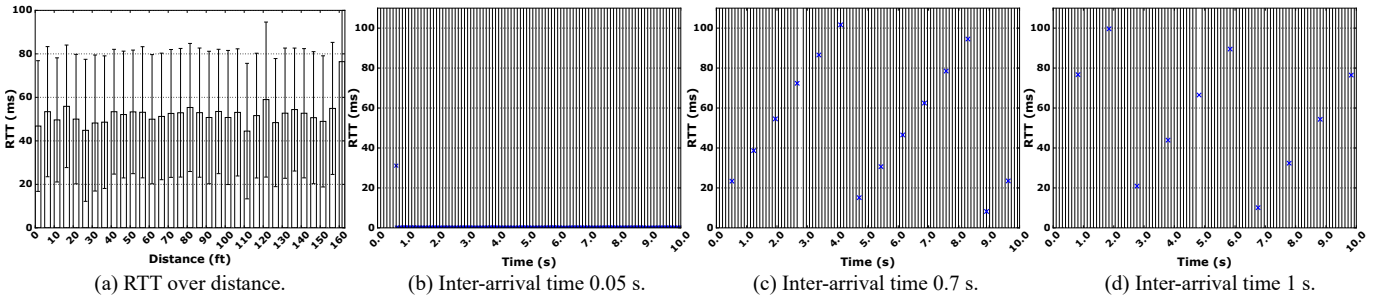


Fig. 10. Variation of RTT with distance (a) and packet inter-arrival time (b, c, d).

itself instead of the desktop host behind the router, removing the possibility of a delayed REPLY from the end-host. Our observations were similar confirming that delays are caused in the 802.11ad wireless path.

To understand the underlying cause, we went back to the original setup, but we now captured the packets at both the wired and wireless interfaces. Careful analysis of the packet traces revealed that ICMP REPLY packets were *held-up* at the AP before being transmitted over the 802.11ad interface for almost the entire RTT measured by the ping program. Further, when we reversed the ping's direction (from the desktop connected to the AP to the laptop), the ICMP REQUEST packets suffered the same hold-up as experienced by the ICMP REPLY packets before. We further found that the amount of extra delay experienced by the ICMP packets was always equal to time between the arrival of the ICMP REQUEST/REPLY at the AP and the *next 802.11ad's DMG beaconing start*. The 802.11ad DMG beaconing for our APs occurs every 102.4 ms and takes about 0.6 ms to complete. We made two observations: (i) Packets are held at the AP regardless of their arrival time, hence, the added delay can be as long as 103 ms (if a packet arrives right after the completion of a DMG beaconing and is held up until the next DMG beaconing). (ii) Among all packets arriving at the router at a given amount of time before the next DMG beaconing, only a fraction of them experiences the RTT inflation, while others are transmitted immediately. These two observations together explain the large

standard deviations in Figure 10(a). However, they also suggest that there is another logic explaining the packet hold up and the resulted RTT inflation.

We suspected a logic that prefers delaying packets at the AP in the anticipation of higher aggregation. To explore this, we varied the interval between consecutive pings from 0.01 s to 1 s and measured the RTTs. Figures 10(b), 10(c) and 10(d) plot the RTT of consecutive pings sent with an inter-arrival time of 0.05, 0.7 and 1.0 s, respectively. The vertical lines mark the beginning of a DMG beaconing. For the 0.05 s case, surprisingly there is no RTT inflation (except for the very first packet). In fact, we observed the exact same behavior for all inter-arrival times shorter than 0.1024 s. On the other hand, pings with inter-arrival times longer than 0.1024 s suffer inflated RTT which seems to follow a distinct pattern. For example, see Figure 10(c) for the 0.7 s case; the first packet has RTT of about 20 ms, the second one about 40ms and so on. However, after the increasing value of RTT reaches about 100 ms, the next packet's RTT goes back to 20 ms. Note that 100 ms is very close to the beaconing period of 102.4 ms. We observe a similar pattern for the 1.0 s case in Figure 10(d). This zig-zag pattern of the RTT inflation further explains why we observed large variations in RTT in our original experiments. Unfortunately, we were not able to explain the logic behind this pattern, which seems to be the result of a complex interplay among the packet inter-arrival time, the beaconing period, and AP-internal counters/timers

governing packet transmission.

Note that this RTT inflation does not affect the throughput of backlogged transfers, where the packet inter-arrival times are much shorter than 0.1024 s. However, this observation has a significant implication for non-backlogged traffic. We verified that this RTT inflation is experienced by TCP packets as well, suggesting that many applications can be affected. For example, page load times in web access would be artificially inflated because of this behavior, as the first RTT (for the SYN-SYNACK exchange in this case) always experiences inflation (Figure 10(b)).

VI. SPATIAL SHARING

The order-of-magnitude shorter wavelengths in mmWave bands compared to the 2.4/5 GHz bands makes it possible to pack a very large number of antenna arrays into small form factors, enabling highly directional transmissions. Directional communication allows for spatial reuse i.e. the ability to establish multiple concurrent transmission links at the same time without interfering with each other. However, generating pencil directional beams with minimum side lobes requires complex phased antenna array design with large number of antenna elements. In contrast, all COTS 802.11ad enabled devices use a simple phased antenna array architecture with 32 antenna elements at most. As a result, the constructed beams are not very directional and have many side lobes leading to the following questions: how many parallel links can we establish using COTS devices without degrading single link performance? How far should these links be from each other to allow for spatial sharing and experience small performance degradation?

To answer these questions, we conduct different sets of experiments to cover multiple deployment scenarios in the real world. In each experiment, we have two pairs of wireless links (referred to as “left” and “right” link) operating in the same frequency channel. Each pair consists of a single client and a single AP and each AP broadcasts a unique SSID. The AP and its corresponding client are placed very close to each other creating a strong link. Both clients start a TCP session towards their peer APs (uplink scenario). For each experiment, we change the placement and the direction of the communication to one of the following topologies: i) Parallel vertical links ($\uparrow\uparrow$), ii) vertical and horizontal links ($\uparrow\rightarrow$), iii) horizontal links ($\rightarrow\leftarrow$). For each topology, the arrow shows the direction of communication from the client to the AP. For example, in topology (iii), the two clients face each other and the two APs are between them, each facing towards its own client but away from each other. Frame aggregation is set to the maximum level allowed by the firmware.

We study the impact of operating two links in the same frequency channel on the perceived throughput¹ for various values of separation distances between the two links. We start our measurement by shifting the right link with a resolution

¹Each link is capable of achieving around 1.6 Gbps of throughput during standalone operation.

distance of 40 cm towards the left link. At each distance, we run 10 iPerf sessions, each lasting for 60 seconds, and we plot the average aggregated application throughput with a confidence interval of 95%.

Figure 11 depicts the aggregated throughput for the two links with respect to separation distance. As expected, higher separation distance results in a higher aggregated throughput for the different placements. On the other hand, the smaller the separation distance becomes, the higher the probability the two pairs can sense each other and, as a result, start sharing the wireless medium. The high variation of the throughput is due to many factors: the proprietary rate adaptation algorithm, the contribution of reflections inside the measurement area, and the beam selection algorithm.

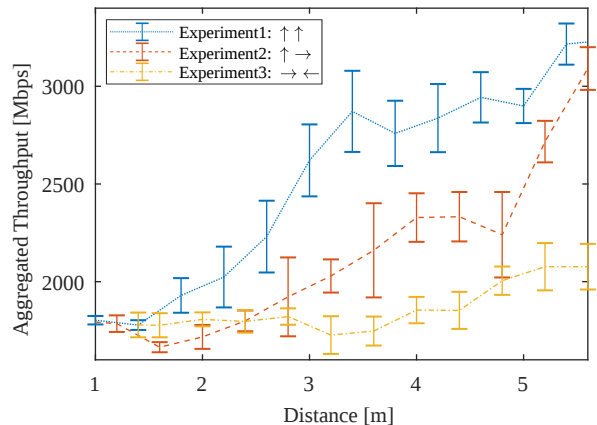


Fig. 11. Spatial sharing performance for two links in different placements.

The topology of two horizontal links performs the worst in terms of aggregated throughput compared to the other two topologies. This is due to the fact that the two clients can hear each others transmissions and thus defer their own transmissions. On the other hand, the topology of two vertical links allows for the maximum spatial reuse and provides the best aggregate throughput for any separation distance. When the separation distance is longer than 5.6 m, each client can achieve around 1.6 Gbps, same as in standalone operation. However, for shorter separation distances, the two links start interfering with each other via their side lobes. Between 3.6 m and 4.2 m, the aggregated throughput decreases by an amount of 400 Mbps and remains around 2.8 Gbps. For further shorter separation distances, the aggregated throughput starts to decrease proportionally with the separation distance. Finally, the performance in topology (ii) is better than in the horizontal topology, as in this case side-lobe interference is not as strong, but worse than in the vertical topology.

Overall, we observe that COTS devices do not always allow for high spatial reuse due to the use of wide beam patterns and side lobes. Figure 12 depicts two antenna patterns that the Talon router uses, taken from [4]. As can be seen, the Talon router uses a single beam pattern for reception which has quasi-omni shape in the azimuth plane. In addition, it frequently uses sector (20) which has a strong lobe when

facing the peer station but also has many side lobes. Thus, the wide beam of the receive sector and the strong side lobes in each transmit sector used by the Talon router [4] explain the need for a large separation distance between parallel links to achieve a high degree of spatial reuse. Additionally, the orientation of links has a strong impact. For certain orientations, mmWave links can operate similarly to wired networks, whereas for other orientations, interference is similar to the case of traditional wireless networks. This is a unique feature of mmWave networks. Traditional protocols for wired and/or wireless networks are not designed for this behavior.

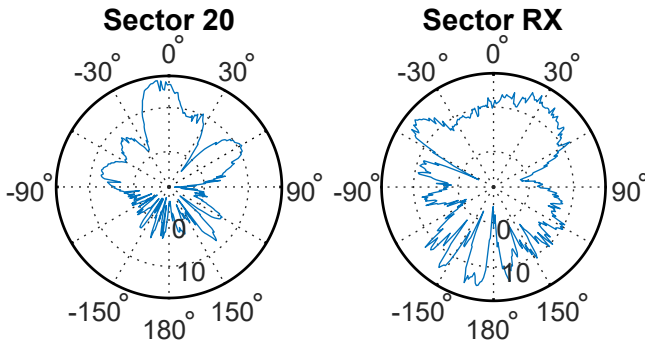


Fig. 12. Two antenna radiation patterns in azimuth plane [4].

VII. DISCUSSION

After analyzing the performance of the COTS 802.11ad devices, we got some insights into the existing problems in those devices so we discuss some of the possible solutions.

Phased Antenna Array. Both the Talon and the NightHawk routers use a phased antenna array of 32 antenna elements that implement analog beamforming. In [4], the authors measured the 2D radiation patterns of the sectors defined in the codebook of the Talon router in an anechoic chamber. All the sectors have irregular and non-directional patterns. However in theory, a linear phased antenna array of 32 elements can generate very narrow beams with a beamwidth of 7 degrees assuming the elements are spaced by a half lambda. However, the antenna array used in those devices arrange the elements in an asymmetric way where some of the elements are located on the surface of the antenna module while others are located on the back and the rest are located on the sides of the board. This arrangement results in irregular beam patterns. The wide irregular beams are good for robust communication during user mobility within an indoor environment. This is because the device does not have to continuously sweep across all its sectors to avoid link interruption thus resulting in a smooth experience to the end user. In addition, since those devices are limited for indoor usage with few number of devices, it makes sense to use wide beams for mobility and robustness. In addition, those devices work well enough with those beam patterns as they can achieve Gbps throughput across the room except for the blockage case. However, as network becomes dense and we try to maximize the number

of clients, interference increases significantly. Thus, achieving spatial reuse becomes hard. Another problem that exacerbates in the mmWave band is that antenna arrays require precise calibration during the manufacturing process so that they can operate as expected. Since this is a complex process that mandates a lot of measurements to characterize the antenna array and its elements, many vendors may eliminate this step as it would increase the cost of end devices. As a result, this may make end devices of the same manufacturer have different and unpredicted performance [20]. Thus one can anticipate that the commercial low end devices in the future will exhibit similar performance to those routers. On the other hand, future devices will most likely integrate multiple phased antenna array to overcome the blockage case [21].

Beamforming. As mentioned earlier, the current 802.11ad off-the-shelf devices implements analog beamforming in which a single RF chain is connected to all the antenna elements. To steer the antenna into a specific direction in space, we modify the excitation, i.e., the phase and the amplitude of each element. The current firmware provides this capability. It allows the end user to configure the beam patterns and modify the weighting network that controls the antenna elements, thus generating relatively narrow beam patterns as opposed to the default beams defined in the codebook of those devices [4]. This allows us to reduce interference which is important for dense deployment and spatial reuse. On the other hand, this is a problem for beamforming training and user tracking with narrow beams. Another possibility to generate narrow beams would be by using different beamforming architectures such as a hybrid beamforming architecture [22], [23]. The hybrid beamforming provides similar performance to digital beamforming but with lower complexity and less power consumption.

COTS Firmware. The current firmware running on Qualcomm 11ad chipsets exposes some Netlink commands to the user space to control the chipset and query information regarding network operation. However, it neither provides a capability to modify the rate control mechanism nor change the logic of sector selection after the beamforming training phase. This is important as the algorithmic part of those mechanisms change based on the deployment scenario. For example, deploying 802.11ad network in a busy place such as mall with dense and high user mobility requires fast beam tracking and rate adaptation algorithms to ensure smooth experience and avoid frequent link blockage. Whereas, deploying 802.11ad network in an office environment where human mobility is not a concern, allows the usage of low-complex algorithms.

Channel Access Schemes. We showed in Section III the impact due to the interaction between CSMA/CA and TCP for different TCP buffer sizes on network throughput and delay when using CSMA/CA with a variable number of stations. The 802.11ad standard introduces hybrid medium access which compromises both contention based access (CSMA/CA) and time based access (TDMA). Both the idle time and the contention in CSMA/CA have high impact on TCP performance and fairness. In addition to that, we have deafness issues which did not exist in omni-directional

communications. On the other hand, a time based channel access scheme improves fairness and network efficiency and guarantees QoS but requires a complex resource scheduling algorithm. The current firmware only supports CSMA/CA channel access and guarantees QoS through the Enhanced distributed channel access (EDCA).

AP Deployment. In our study, we focus on transport and MAC layer aspects for a network with a single AP and multiple devices located at the same height within close proximity of each other. Although this setup allows us to isolate the effect of deafness, AP orientation, and placement within the room, it does not reflect a realistic deployment. A realistic deployment would incorporate multiple APs distributed across a large area where each AP is mounted on the ceiling and pointing towards a certain direction. The authors in [4], [14] measured the 3D beam patterns for the Talon routers and they found that some of the beams were directional in the 3D space at a certain azimuth and elevation angles. The authors in [24] perform an extensive measurement campaign to understand how to deploy COTS mmWave AP to achieve the best coverage and throughput. These two studies encourage further research to understand how to efficiently place many APs to achieve high spatial reuse, optimize AP and client association, and reduce interference among clients.

VIII. RELATED WORK

60 GHz Practical Work. Related work studies the performance of practical 60 GHz networks using both custom hardware platforms such as software-defined radios [25], [26], [27], and commercial off-the-shelf devices [3], [5], [28], [29]. The former are typically limited in terms of bandwidth and focus on the physical layer only, thus not allowing for an analysis of upper-layer issues such as in this paper. The latter use pre-standard 60 GHz devices that do not allow for networking and thus typically study individual links only. While such papers analyze the performance of TCP on mmWave links and emulate the deployment of multiple APs [3], [6], [30], the lack of multiple stations and a backbone network strongly limits their insights compared to our analysis.

mmWave MAC Layer. Medium access control plays a fundamental role on the alleged “pseudo-wired” behavior of mmWave links. Earlier work studies its performance both analytically [31] and in simulation [32]. While 802.11ad allows for multiple access based on time-division [8], [33], existing hardware implements CSMA/CA only. The key problem of CSMA/CA in directional mmWave networks is deafness. Related work suggests virtual carrier sensing [34], [35] to address this issue. However, practical work on 802.11ad devices shows that spatial sharing is limited due to the highly irregular beampatterns of commercial off-the-shelf devices [3]. In contrast to the above earlier work, we are the first to study the medium sharing behavior of 802.11ad in practice.

Frame Aggregation. Due to the large bandwidth available in the 60 GHz band, frame aggregation has a particularly large impact on the throughput performance of 802.11ad [36]. While WiFi networks operating at lower frequencies must

generate frame sizes in the order of milliseconds to achieve significant gains [37], [38], [39], 802.11ad aggregation in the order of microseconds results in even larger gains [3]. Still, the challenges of frame aggregation at low frequency [40], [41] are often valid also for higher frequencies. For instance, related work shows that high levels of aggregation increase packet error rates in 802.11n/ac [42], [43], [39]. We extend this analysis for the case of 802.11ad.

IX. CONCLUSION

We study protocol aspects of the MAC layer and TCP in practical mmWave networks. In contrast to earlier work, we consider a complete IEEE 802.11ad network with one AP and up to eight stations. We perform our analysis on a practical testbed using commercial off-the-shelf hardware. Our results show that dynamic TCP buffer sizing is crucial in the uplink because the multi-gigabit-per-second speeds at the physical layer exacerbate the inefficiencies of CSMA/CA. Further, we show the impact of link orientation on spatial sharing and the limitations of frame aggregation. Regarding delay, we find that the regular beacon transmission process of IEEE 802.11ad APs can inflate the round trip time, thus degrading performance. Overall, we conclude that the characteristics of mmWave links do neither match the behavior of wired nor traditional wireless links.

X. ACKNOWLEDGMENTS

This work has been supported in part by the ERC project SEARCHLIGHT grant no. 617721, the Ramon y Cajal grant RYC-2012-10788 and the Madrid Regional Government through the TIGRE5-CM program (S2013/ICE-2919). Further, this work was supported in part by NSF grant CNS-1553447.

REFERENCES

- [1] R. Mudumbai, S. K. Singh, and U. Madhow, “Medium access control for 60 GHz outdoor mesh networks with highly directional links,” in *IEEE INFOCOM 2009*, 2009, pp. 2871–2875.
- [2] Y. Tian, K. Xu, and N. Ansari, “Tcp in wireless environments: problems and solutions,” *IEEE Communications Magazine*, 2005.
- [3] T. Nitsche, G. Bielsa, I. Tejado, A. Loch, and J. Widmer, “Boon and Bane of 60 GHz Networks: Practical Insights into Beamforming, Interference, and Frame Level Operation,” in *Proc. of CoNEXT’15*, 2015.
- [4] D. Steinmetzer, D. Wegemer, M. Schulz, J. Widmer, and M. Hollick, “Compressive millimeter-wave sector selection in off-the-shelf IEEE 802.11ad devices,” in *13th International Conference on emerging Networking EXperiments and Technologies (CoNEXT 2017)*, 2017.
- [5] Y. Zhu, Z. Zhang, Z. Marzi, C. Nelson, U. Madhow, B. Y. Zhao, and H. Zheng, “Demystifying 60GHz outdoor picocells,” in *Proceedings of the 20th Annual International Conference on Mobile Computing and Networking*, 2014.
- [6] S. K. Saha, A. Garg, and D. Koutsonikolas, “A first look at tcp performance in indoor IEEE 802.11 ad WLANs,” in *2015 IEEE Conference on Computer Communications Workshops (INFOCOM WKSHPS)*, 2015.
- [7] S. K. Saha, V. V. Vira, A. Garg, and D. Koutsonikolas, “A Feasibility Study of 60 GHz Indoor WLANs,” in *Proc. of IEEE ICCCN*, 2016.
- [8] IEEE, “Wireless LAN Medium Access Control (MAC) and Physical Layer (PHY) Specifications Amendment 3: Enhancements for Very High Throughput in the 60 GHz Band,” *IEEE Std 802.11ad-2012*, 2012.
- [9] “Lede project.” [Online]. Available: <https://lede-project.org/>
- [10] T. Li, D. Leith, and D. Malone, “Buffer sizing for 802.11-based networks,” *IEEE/ACM Trans. Netw.*, vol. 19, no. 1, 2011.
- [11] “Tp-link talon ad7200 multi-band wi-fi router.” [Online]. Available: http://www.tp-link.com/us/products/details/cat-5506_AD7200.html

- [12] "Netgear Nighthawk® X10." <https://www.netgear.com/landings/ad7200>.
- [13] Acer *TravelMate P446-M*. [Online]. Available: <https://www.acer.com/ac/en/US/content/professional-series/travelmatep4>
- [14] D. Steinmetzer, D. Wegemer, and M. Hollick. (2017) Talon tools: The framework for practical ieee 802.11ad research. [Online]. Available: <https://seemoo.de/talon-tools>
- [15] M. Maity, B. Raman, and M. Vutukuru, "Tcp download performance in dense wifi scenarios," in *7th International Conference on Communication Systems and Networks (COMSNETS)*, 2015.
- [16] G. Kuriakose, S. Harsha, A. Kumar, and V. Sharma, "Analytical models for capacity estimation of ieee 802.11 w lans using dcf for internet applications," 2009.
- [17] M. A. Ergin, K. Ramachandran, and M. Gruteser, "An experimental study of inter-cell interference effects on system performance in unplanned wireless lan deployments." Elsevier North-Holland, Inc., 2008.
- [18] R. Bruno, M. Conti, and E. Gregori, "Modeling tcp throughput over wireless lans," 2015.
- [19] X. Liu, F. Ren, R. Shu, T. Zhang, and T. Dai, "Mitigating bufferbloat with receiver-based tcp flow control mechanism in cellular networks." [Online]. Available: https://nns.cs.tsinghua.edu.cn/paper/icccn15_xll.pdf
- [20] "Challenges and Techniques for Characterizing Antenna Systems for 5G." [Online]. Available: https://www.nttdocomo.co.jp/binary/pdf/corporate/technology/rd/tech/5g/5GTBS2017_TECH_WORKSHOP_R&S.pdf
- [21] "The promise of 5g mmwave how do we make it mobile?" [Online]. Available: <https://www.qualcomm.com/media/documents/files/the-promise-of-5g-mmwave-how-do-we-make-it-mobile.pdf>
- [22] A. Alkhateeb, O. E. Ayach, G. Leus, and R. W. Heath, "Channel estimation and hybrid precoding for millimeter wave cellular systems," *IEEE Journal of Selected Topics in Signal Processing*, 2014.
- [23] J. Palacios, D. D. Donno, D. Giustiniano, and J. Widmer, "Speeding up mmwave beam training through low-complexity hybrid transceivers," in *2016 IEEE 27th Annual International Symposium on Personal, Indoor, and Mobile Radio Communications (PIMRC)*, 2016.
- [24] S. Kumar Saha¹, H. Assasa, A. Loch, N. Muralidhar Prakash¹, R. Shyamsunder¹, S. Aggarwal¹, D. Steinmetzer, D. Koutsonikolas¹, J. Widmer, and H. Matthias, "Fast and infuriating: Performance and pitfalls of 60 ghz w lans based on consumer-grade hardware," in *IEEE International Conference on Sensing, Communication and Networking (SECON)*, 2018.
- [25] S. Sur, V. Venkateswaran, X. Zhang, and P. Ramanathan, "60 GHz Indoor Networking Through Flexible Beams: A Link-Level Profiling," in *Proceedings of the 2015 ACM SIGMETRICS International Conference on Measurement and Modeling of Computer Systems*, 2015.
- [26] J. Zhang, X. Zhang, P. Kulkarni, and P. Ramanathan, "Openmili: A 60 ghz software radio with a programmable phased-array antenna: Demo," in *Proceedings of the 22Nd Annual International Conference on Mobile Computing and Networking*, 2016.
- [27] X. Tie, K. Ramachandran, and R. Mahindra, "On 60 GHz Wireless Link Performance in Indoor Environments," in *Proceedings of the 13th International Conference on Passive and Active Measurement*, 2012.
- [28] S. K. Saha, T. Siddiqui, D. Koutsonikolas, A. Loch, J. Widmer, and R. Sridhar, "A detailed look into power consumption of commodity 60 ghz devices," in *2017 IEEE 18th International Symposium on A World of Wireless, Mobile and Multimedia Networks (WoWMoM)*, 2017.
- [29] Y. Zhu, X. Zhou, Z. Zhang, L. Zhou, A. Vahdat, B. Y. Zhao, and H. Zheng, "Cutting the cord: A robust wireless facilities network for data centers," in *Proceedings of the 20th Annual International Conference on Mobile Computing and Networking*, 2014.
- [30] S. K. Saha, V. V. Vira, A. Garg, and D. Koutsonikolas, "Multi-gigabit indoor w lans: Looking beyond 2.4/5 ghz," in *2016 IEEE International Conference on Communications (ICC)*, 2016.
- [31] K. Chandra, R. V. Prasad, and I. Niemegeers, "Performance analysis of ieee 802.11ad mac protocol," *IEEE Communications Letters*, vol. 21, no. 7, 2017.
- [32] X. Zhu, A. Doufexi, and T. Kocak, "Throughput and coverage performance for ieee 802.11ad millimeter-wave w lans," in *2011 IEEE 73rd Vehicular Technology Conference (VTC Spring)*, May 2011, pp. 1–5.
- [33] J. Qiao, X. Shen, J. W. Mark, Z. Shi, and N. Mohammadzadeh, "Mac-layer integration of multiple radio bands in indoor millimeter wave networks," in *2013 IEEE Wireless Communications and Networking Conference (WCNC)*, 2013.
- [34] M. X. Gong, D. Akhmetov, R. Want, and S. Mao, "Multi-user operation in mmwave wireless networks," in *2011 IEEE International Conference on Communications (ICC)*, 2011.
- [35] M. X. Gong, R. Stacey, D. Akhmetov, and S. Mao, "A directional csma/ca protocol for mmwave wireless lans," in *2010 IEEE Wireless Communication and Networking Conference*, 2010.
- [36] H. Assasa, A. Loch, and J. Widmer, "Packet mass transit: Improving frame aggregation in 60 ghz networks," in *2016 IEEE 17th International Symposium on A World of Wireless, Mobile and Multimedia Networks (WoWMoM)*, 2016.
- [37] D. Skordoulis, Q. Ni, H. h. Chen, A. P. Stephens, C. Liu, and A. Jamalipour, "Ieee 802.11n mac frame aggregation mechanisms for next-generation high-throughput w lans," *IEEE Wireless Communications*, vol. 15, no. 1, 2008.
- [38] B. Ginzburg and A. Kesselman, "Performance analysis of a-mpdu and a-msdu aggregation in ieee 802.11n," in *2007 IEEE Sarnoff Symposium*, 2007.
- [39] S. Byeon, K. Yoon, O. Lee, S. Choi, W. Cho, and S. Oh, "Mofa: Mobility-aware frame aggregation in wi-fi," in *Proceedings of the 10th ACM International on Conference on Emerging Networking Experiments and Technologies*, 2014.
- [40] A. Majeed and N. B. Abu-Ghazaleh, "Packet aggregation in multi-rate wireless lans," in *2012 9th Annual IEEE Communications Society Conference on Sensor, Mesh and Ad Hoc Communications and Networks (SECON)*, 2012, pp. 452–460.
- [41] B. Bellalta, J. Barcelo, D. Staehle, A. Vinel, and M. Oliver, "On the performance of packet aggregation in ieee 802.11 ac mu-mimo w lans," *IEEE Communications Letters*, vol. 16, no. 10, pp. 1588–1591, 2012.
- [42] A. Saif and M. Othman, "A reliable a-msdu frame aggregation scheme in 802.11n wireless networks," *Procedia Computer Science*, vol. 21, 2013.
- [43] A. Saif, M. Othman, S. Subramaniam, and N. A. W. A. Hamid, "An enhanced a-msdu frame aggregation scheme for 802.11n wireless networks," *Wireless Personal Communications*, vol. 66, no. 4, pp. 683–706, Oct 2012.